DOI: 10.1002/ejic.200800595

Dynamic Stereochemical Behaviour of Congested Ruthenium(II) Complexes Containing Asymmetric Thioether Ligands Based on Pyridine and Pyrimidine

Giuseppe Tresoldi,*[a] Santo Lanza,[a] Santo Di Pietro,[a] and Dario Drommi[a]

Keywords: Ruthenium / Nitrogen heterocycles / Sulfur / N,S ligands / Bridging ligands

The asymmetric thioethers L [L = 2-pyridylmethyl 2′-pyrimidyl sulfide (pps) and 2-(4-methylpyrimidyl) 2′-pyridylmethyl sulfide (mps)] reacted with *cis*-[$RuCl_2(N,N\text{-}L')_2$] [L′ = di-2-pyridyl sulfide (dps); 2,2′-bis(4-methylpyridyl) sulfide (4mdps); 2,2′-bis(5-methylpyridyl) sulfide (5mdps)] to give the five-membered-ring chelate complexes [$Ru(N,N\text{-}L')_2(N_{pyridine},S\text{-}L)]^{++}$ as the major products (92–95 %). Because the sulfur and ruthenium atoms are stereogenic centres, with (*R*) and (*S*) and Δ and Λ configurations, respectively, four isomers, including the enantiomers were obtained. At low temperature and in the methylene region of the ^1H NMR spectra, two AB systems due to the enantiomer couples Δ*S* Λ*R* (**a**) and Δ*R* Λ*S* (**b**) were observed with abundances of 77–89 and 6–18 %, respectively. Furthermore, NMR spectroscopic investigations showed that the hybrid polydentate ligands L change their coordination mode. Thus, although **a** and **b** largely predominate, a mixture of species containing L and the $Ru(N,N\text{-}L')_2$ unit in the ratio 1:1 are present. The four-membered-ring chelate complexes $[Ru(N,N\text{-}L')_2(N_{pyrimidine},S\text{-}L)]^{++}$ (**c**), as minor species (abundance 1–8 %), are always observed, whereas the dinuclear species $[\{Ru(N,N\text{-}L')_2\}_2(\mu\text{-}L)_2]^{+4}$ (**d**, **e**) are observed when L′ = dps or 5mdps. In these cases, four AB systems are assigned to dinuclear species **d** and **e** containing two bridging L that act as $N_{pyridine}$,S- or $N_{pyridine}$, $N_{pyrimidine}$-donor ligands. The ^1H NMR spectra are temperature dependent in that at low temperature the complexes undergo inversion of the chiral centre of the coordinated sulfur atom (**a** ⇌ **b**) and the dimer (**d**, **e**) and monomer (**c**) are in equilibrium; at higher temperatures the complexes undergo a structural dynamic rearrangement, which involves exchange between the coordinated and uncoordinated N atoms (**b** ⇌ **c**). One-dimensional band-shape analysis of the exchanging methylene and methyl proton signals showed that the energy barriers for inversion of the sulfur centre are in the 50–53 kJ mol^{-1} range, whereas those for the higher-temperatures process are in the 62–68 kJ mol^{-1} range. The possible mechanisms of the processes are discussed. NMR spectroscopic findings suggest that inversion at the sulfur centre occurs without any bond rupture, whereas the exchange, at higher temperatures (**b** ⇌ **c**), is a dissociative process involving the breaking of a Ru–$N_{pyridine}$ bond.

Introduction

Polydentate ligands can adopt a variety of bonding modes depending on the denticity of the ligand itself and the nature of the metal moiety to which it is coordinated.[1] On the other hand, the bonding modes of the polydentate ligands can promote stereochemical nonrigidity of the transition-metal complexes.[2–4] Dynamic stereochemical rearrangements can be observed if all of the donor groups coordinated, but it can occur reversibly in an on/off coordination mode for one of the donor groups.[4,5] In contrast, if at least one donor atom remains uncoordinated, it is possible to observe the exchange between different coordination modes. When tridentate ligands such as 2,2′:6,2′′-terpyridine bond in a bidentate mode they display dynamic behaviour that involves exchange between the pendant and the coordinated ring.[3–7] Sometimes, restricted rotation of the pendant ring is observed.[3,7,8] Hybrid ligands often display dynamic behaviour.[5] In particular, tridentate sulfur–nitrogen ligands, if restricted to the bidentate bonding mode, show, in addition to inversion of the coordinated sulfur,[9] exchange between the coordinated and uncoordinated sulfur atom.[10] Mechanisms proposed for the exchange between coordinated and uncoordinated donor atoms include the "tick–tock twist" mechanism, which involves a pseudo-tridentate bonding mode of the ligand in the transition state, the "rotation" mechanism, which involves the loosening of the outer metal-donor atom bond followed by a 180° rotation about the central metal-donor atom bond, and a mechanism involving cleavage of the outer metal-donor atom bond followed by the formation of a T-shaped intermediate, in which the polydentate ligand is bound to the metal in a monodentate fashion.[4,6–8,11]

Some years ago, studying the coordination chemistry of thioethers based on pyridine or pyrimidine, we found that these usually N,N-bidentate donors[12] often show N,S che-

[a] Dipartimento di Chimica Inorganica, Chimica Analitica e Chimica Fisica, Università di Messina,
Salita Sperone 31, 98166 Messina, Italy
Fax: +39-090393756
E-mail: gtresoldi@unime.it

Supporting information for this article is available on the WWW under http://www.eurjic.org or from the author.

lation towards congested ruthenium substrates.[13–17] The resultant complexes display dynamic stereochemical rearrangements associated with inversion at the sulfur atom coordinated to the ruthenium,[14] the restricted rotation of the pendant ring[15] and the exchange between different coordination modes.[17] NMR spectroscopic studies by us were performed to elucidate the mechanisms of these processes. Inversion of the sulfur centre and restricted rotation were studied when potentially bidentate ligands were used,[14,15] whereas the exchange between different coordination modes was observed when thioethers, which are generally asymmetrical and potentially tridentate, were used.[17] In the last case, different types of bonding groups show different bond strengths, and the thioethers may act as hemilabile ligands with dissociation and recoordination of weakly bound groups.

For the compounds[17] $[Ru(N,N\text{-diimmine})_2L^1][PF_6]_2$ [diimmine = 2-pyrimidyl sulfide, 2,2′-bis(5-ethylpyrimidyl) sulfide; L^1 = 2-pyridylmethyl 2′-pyridyl sulfide, 2-pyridylmethyl 2′-pyrimidyl sulfide (pps) and 2-(4-methylpyrimidyl) 2′-pyridylmethyl sulfide (mps)] only two exchanging species were observed. In the major species, L^1 was $N_{pyridine}$,S-chelated, and in the minor species, L^1 was $N_{pyridine}$ monodentate. Furthermore, NMR spectroscopic findings supported a mechanism for the exchange between the two species involving the formation of a labile N,N-chelated intermediate.

This paper explores the nature and the dynamic behaviour of the species present in the mixtures obtained by reaction of pps and mps with $RuCl_2(N,N\text{-dps})_2$ (**1** and **2**, respectively), $RuCl_2(N,N\text{-4mdps})_2$ (**3** and **4**) and $RuCl_2(N,N\text{-5mdps})_2$ (**5** and **6**) [dps = di-2-pyridyl sulfide, 4mdps = 2,2′-bis(4-methylpyridyl) sulfide, 5mdps = 2,2′-bis(5-methylpyridyl) sulfide] and the mechanisms of the exchange processes. The structure of $[Ru(N,N\text{-dps})_2(N,S\text{-mps})][PF_6]_2$ is already reported.[16]

Results

Synthesis of the Compounds

The yellow or orange air-stable solids **1**–**6** were obtained by the reactions of *cis*-$[RuCl_2(N,N\text{-L}')_2]$ and L and as depicted in Scheme 1. Although the $[Ru(N,N\text{-L}')_2(N_{pyridine},S\text{-L})][PF_6]_2$ (**a**, **b**) species largely predominate, a mixture of mono- and dinuclear species are present that also contain species **c**, **d** and **e**.

These compounds, soluble in acetone or acetonitrile, were characterized by elemental analysis, conductivity measurements in acetonitrile solutions (values in the range 320–350 $S\,cm^2\,mol^{-1}$) and IR spectroscopy, which shows the bands of PF_6^- (ca. 844 and 558 cm^{-1}) and those characteristic of thioether ligands in the range (1630–1540 and 780–720 cm^{-1}). These data indicate that dps, 4mdps and 5mdps act as N,N-chelate ligands.[12–17] These findings were confirmed by subsequent ^1H and ^{13}C NMR spectroscopic studies.

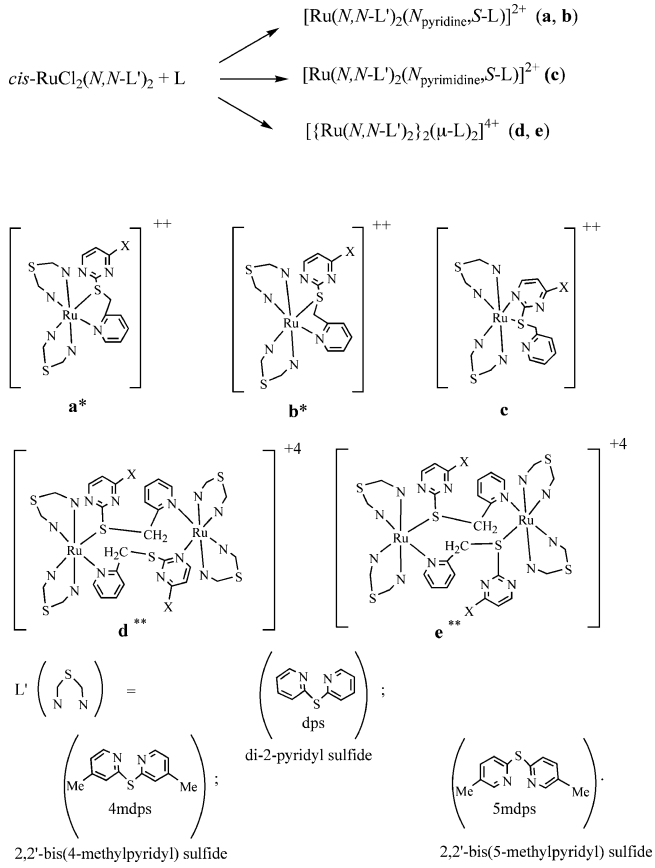

Scheme 1. X = H, L = 2-pyridylmethyl 2′ pyrimidyl sulfide (pps); X = Me, L = 2-(4-methylpyrimidyl) 2′-pyridylmethyl sulfide (mps); * the invertomer **a** has the configuration Δ*S* and Λ*R*, **b** Δ*R* and Λ*S*. ** proposed structure of dinuclear species (**d**, **e**) observed when L′ = dps or 5mdps.

Dynamic NMR Spectroscopic Studies

Variable-temperature ^1H NMR spectra of the compounds were obtained in $(CD_3)_2CO$ in the range 200–330 K. At low temperature, the ^1H NMR spectra and the COSY and EXSY experiments performed on solutions of the complex showed the presence of two, slow-exchanging, mononuclear invertomers of the formula $[Ru(N,N\text{-L}')_2(N_{pyridine},S\text{-L})][PF_6]_2$ (**a**, **b**) and a nonexchanging species $[Ru(N,N\text{-L}')_2(N_{pyrimidine},S\text{-L})][PF_6]_2$ (**c**, abundance 1–8%). In some cases the two dinuclear species $[\{Ru(N,N\text{-L}')_2\}_2(\mu\text{-L})_2][PF_6]_4$ (**d**, **e**; abundance 0–3%) were also observed.

The ^1H NMR spectroscopic data for the methylene group of **1**–**6** are listed in Table 1. Identification of the protons was performed by COSY, NOESY and decoupling experiments and by comparing the spectra at different temperature. Specific regions of the ^1H NMR spectrum of **6** at 208 K are depicted in Figure 1a,b (aromatic and methyl regions) and Figure 2 (methylene region).

All the aromatic signals of major invertomer **6a** and some signals of minor invertomer **6b** are labelled in Figure 1a. In particular, the L pyridine proton signals (ring A) of **6a** are observed at δ = 9.25 (H^6), 7.93 (H^4), 7.53 (H^5), 7.47 (H^3) ppm and the methylpyrimidine signals (ring B) at

Table 1. ^{1}H NMR spectroscopic data in the methylene region.[a]

Compound	T / K	%	$\delta(CH_2)$ / ppm		J_{CH_2} / Hz	Compound	T / K	%	$\delta(CH_2)$ / ppm		J_{CH_2} / Hz
pps	298[b]		4.54			**mps**	298[b]		4.52		
1a	218[b]	88.2	4.82	3.80	17.0	**2a**	223[b]	84.0	4.75	3.74	16.8
1b		6.5	5.08	3.93	14.7	**2b**		8.0	5.03	3.88	14.8
1c		2.0	6.61	5.74	18.8	**2c**		6.0	6.59	5.74	18.8
1d		2.5	5.76	5.43	17.2	**2d**		1.0	5.80	5.46	17.0
			5.20	3.58	17.0				5.18	3.53	17.0
1e		0.8	5.98	5.26	18.0	**2e**		1.0	6.08	5.24	18.2
			5.32	4.36	16.1				5.28	4.38	16.2
1a + 1b	313[b]	94.7	4.75	3.73	16.6	**2a + 2b**	313[b]	92.0	4.71	3.72	16.4
1c		5.3	6.55	5.75	18.2	**2c**		8.0	6.57	5.73	18.6
3a	225	86.0	4.77	3.74	16.6	**4a**	228	84.0	4.71	3.69	16.8
3b		9.0	5.05	3.89	14.4	**4b**		8.0	5.02	3.86	14.8
3c		5.0	6.50	5.66	18.2	**4c**		8.0	6.50	5.64	18.5
3a + 3b	313	95,0	4.73	3.72	16.3	**4a + 4b**	313	92.0	4.68	3.70	16.2
3c		5.0	6.46	5.70	18.2	**4c**		8.0	6.49	5.66	17.5
5a	208	77.7	4.72	3.66	16.8	**6a**	208	78.5	4.64	3.62	16.8
5b		17.3	5.04	3.77	14.4	**6b**		15.0	5.02	3.74	14.4
5c		1.5	6.59	5.90	19.0	**6c**		1.5	6.57	5.91	18.8
5d		2.7	5.75	5.41	17.1	**6d**		2.5	5.80	5.43	17.4
			5.16	3.57	16.2				5.14	3.53	16.2
5e		0.8	5.91	5.25	18.2	**6e**		2.5	6.01	5.21	18.2
			5.29	4.36	18.0				5.29	4.41	18.0
5a + 5b	313	95.0	4.75	3.77	16.2	**6a + 6b**	313	94.5	4.68	3.73	16.2
5c		5.0	6.52	5.87	18.9	**6c**		5.5	6.53	5.83	18.2

[a] At 600 MHz unless stated otherwise in [D_6]acetone; δ values reported relative to TMS. [b] 300 MHz.

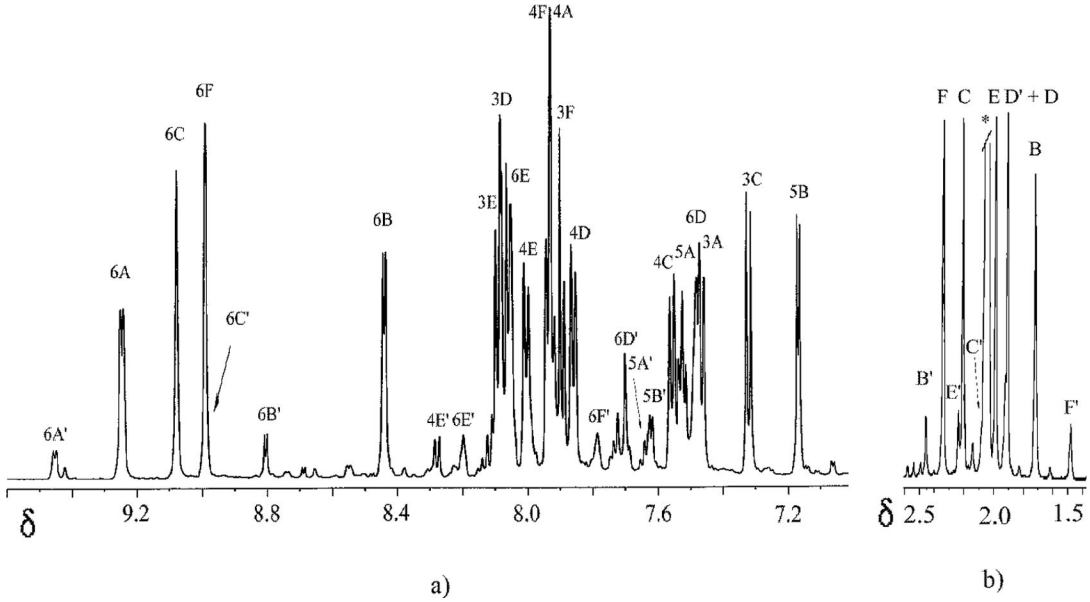

Figure 1. 600 MHz ^{1}H NMR spectrum of **6** in the aromatic region (9.6–6.9 ppm) at 208 K. All the pyridyl and pyrimidyl protons of **6a** are labelled: A (pyridyl ring of L), B (pyrimidyl ring), C (ring *cis* with respect to ring B); C and D are pyridyl rings of the same L ligand; E (ring *trans* with respect to S atom); A′, B′, C′, D′, E′, F′ are the corresponding ring of **6b** (some signals).

δ = 8.44 (H^6), 7.17 (H^5) ppm. The corresponding signals of **6b** are observed at δ = 9.45 (H^6), 7.64 (H^5), 8.08 (H^4), 8.81 (H^6), 7.62 (H^5) ppm (rings A′ and B′, respectively). Moreover, some methylpyrimidine signals of **6c**, **6d** and **6e** not labelled in Figure 1 are assigned: δ = 8.48 (H^6), 7.11 (H^5) ppm for **6c**; δ = 8.55 (H^6), 6.13 (H^5) ppm for **6d**; δ = 8.69 (H^6), 6.54 (H^5) ppm for **6e**.

The methyl signals of major species **6a** (δ = 2.34, 2.20, 1.99, 1.90, 1.72 ppm) and **6b** (δ = 2.46, 2.24, 2.06, 1.92, 1.48 ppm) are assigned in Figure 1b. Moreover, by comparison with the methyl region of the ^{1}H NMR spectrum of **5**, the signals at δ = 2.54, 2.49, 1.49 ppm are assigned to methyl protons of dinuclear species **6d**, and the signals at δ = 2.58, 1.63 ppm are assigned to **6e**.

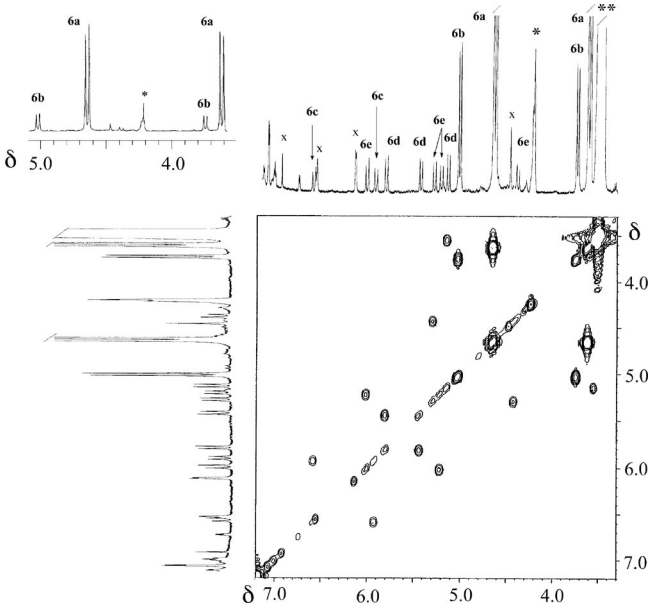

Figure 2. 600 MHz ^{1}H 2D COSY NMR spectrum of **6** at 208 K. Assignments of methylene signals: ^{x}H^5 pyrimidyl signals, * impurity band, ** the solvent band masked the doublet at 3.53 ppm of **6d**. The expansion shows the methylene signals of **6a** and **6b**.

As shown in the 600 MHz ^{1}H 2D COSY NMR spectrum (Figure 2) at 208 K, the methylene region shows 7 AB systems: 3 are assigned to mononuclear species **6a**, **6b** and **6c** and the remaining 4 are assigned to dinuclear species **6d** and **6e**.

At this point, it is important to note that the crystal structure of [Ru(*N*,*N*-dps)$_2$(*N*,*S*-mps)][PF$_6$]$_2$ already reported[16] showed that the compound [Ru(C$_{10}$H$_8$N$_2$S)$_2$-(C$_{11}$H$_{11}$N$_3$S)][PF$_6$]$_2$·C$_2$H$_3$N is composed of a bivalent octahedral Ru^{II} complex, two PF$_6^-$ anions and an acetonitrile solvent molecule. The structure displays a peculiar stereochemistry of the cation. Two N,N-bidentate dps ligands and an N,S-bidentate mps ligand around the Ru centre, together with the coordination of a nonsymmetric S atom, mean that these two atoms are chiral. This would lead to four stereoisomers, but only the enantiomeric pair Δ*S* Λ*R* was found in the analyzed sample.

According to the presence of an invertomer that largely predominates, the COSY experiment (Figure 2) shows two AB doublets of high intensity and two of lower intensity, which are assigned to invertomers **6a** and **6b**, respectively, of the species [Ru(*N*,*N*-5mdps)$_2$(*N*$_{pyridine}$,*S*-mps)][PF$_6$]$_2$ (see expansion of Figure 2 and Table 1). Comparison of the ^{1}H NMR spectra of **1**–**6** shows that the major invertomers **a** all have the configuration Δ*S* Λ*R*. In particular, **6a** is similar to invertomer **2a** of [Ru(*N*,*N*-dps)$_2$(*N*,*S*-mps)][PF$_6$]$_2$.[16] Thus, minor invertomer **6b** has the configuration Δ*R* Λ*S*.

The AB system at δ = 6.57 and 5.91 ppm (J = 18.8 Hz) is assigned to the mononuclear species [Ru(*N*,*N*-5mdps)$_2$-(*N*$_{pyrimidine}$,*S*-mps)][PF$_6$]$_2$ (**6c**). Another four AB systems are observed and assigned to dinuclear compounds **6d** and **6e** of the general formula [{Ru(*N*,*N*-L′)$_2$}$_2$(μ-L)$_2$][PF$_6$]$_4$. Both these species have the same abundance (2.5%) and show four AB doublets due to nonequivalent methylene groups of two bridging L ligands. Unlike **6d** and **6e**, dinuclear compounds **1d** and **1e** (2.5 and 0.8%, respectively) as well as **5d** and **5e** (2.7 and 0.8%, respectively) have different abundances. Furthermore, **2d** and **2e** are in very-low abundance and **3d** and **3e** as well as **4d** and **4e** are not observed. Representations of the proposed structures of **1d**, **2d**, **5d**, **6d** and **1e**, **2e**, **5e**, **6e** are shown in Scheme 1.

All the dinuclear species **d** (see Table 1) exhibit two AB doublets in the methylene region at $\delta \approx$ 5.8, 5.4 ppm with little internal chemical shifts and two AB doublets at $\delta \approx$ 5.1, 3.5 ppm with relatively large internal chemical shifts (see Figure 2). We attribute the last signals to the methylene protons near to the coordinated sulfur atom, as these nuclei will be most sensitive to the configuration of the chiral sulfur atom. In other words, this bridging L ligand is coordinated to the ruthenium atoms with sulfur and N$_{pyridine}$ atoms. Conversely, the signals at δ = 5.8, 5.4 ppm were assigned to methylene atoms near the uncoordinated sulfur atom. Thus, the bridging L ligand is coordinated to the ruthenium atoms with N$_{pyrimidine}$ and N$_{pyridine}$ atoms. Furthermore, although all the signals of the dinuclear species **d** and **e** vanish at ca. 293 K, the signals at $\delta \approx$ 5.8, 5.4 ppm broaden at temperatures lower than those of other AB systems of **d** and **e** suggesting the presence of a weak Ru–N$_{pyrimidine}$ bond.

The dinuclear species **e** exhibit two AB doublets ($\delta \approx$ 6.0, 5.2 ppm and $\delta \approx$ 5.3, 4.5 ppm) in the methylene region with comparable internal chemical shifts ($\Delta\delta$ = 0.8 ppm) according to the presence of two bridging L ligands that are N$_{pyridine}$,S coordinated.

At low temperatures, inversion of the sulfur centre results in interconversions between mononuclear species **6a** and **6b** (Figure 3). Exchanges **a** ⇌ **b** are also observed in EXSY experiments for **1**–**6** at 248 263, 273 and 283 K.

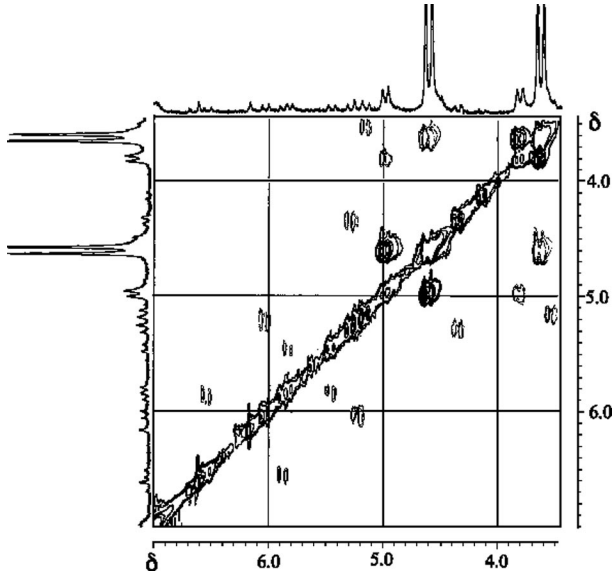

Figure 3. 300 MHz ^{1}H 2D EXSY NMR spectrum in the methylene region of **6** at 263 K.

Table 2. Activation energy data for the fluxional rearrangements of the compounds.

Mixture	Isomers	Process	$\Delta H^{\neq}$ / kJ mol^{-1}	$\Delta S^{\neq}$ / J K^{-1} mol^{-1}	$\Delta G^{\neq}_{298}$ / kJ mol^{-1}
1	**a/b**	Sulfur inversion	49.8 ± 0.4	–1.8 ± 1.5	50.3 ± 0.2
	(a+b)/c	N,N exchange	85.8 ± 1.9	62.2 ± 6.1	67.3 ± 0.3
2	**a/b**	Sulfur inversion	46.2 ± 0.4	–23.4 ± 1.5	53.2 ± 0.1
	(a+b)/c	N,N exchange	115.0 ± 1.0	158.7 ± 1.5	67.7 ± 0.3
3	**a/b**	Sulfur inversion	39.7 ± 0.8	–40.1 ± 2.8	51.6 ± 0.1
	(a+b)/c	N,N exchange	69.1 ± 1.8	22.5 ± 1.5	62.4 ± 0.3
4	**a/b**	Sulfur inversion	51.7 ± 0.7	3.8 ± 2.4	50.6 ± 0.2
	(a+b)/c	N,N exchange	93.1 ± 2.1	96.5 ± 6.8	64.3 ± 0.3
5	**a/b**	Sulfur inversion	41.3 ± 0.5	–33.3 ± 1.9	51.2 ± 0.2
	(a+b)/c	N,N exchange	84.9 ± 2.5	57.2 ± 6.1	67.9 ± 0.6
6	**a/b**	Sulfur inversion	42.6 ± 0.7	–28.6 ± 2.6	51.1 ± 0.1
	(a+b)/c	N,N exchange	81.6 ± 1.9	45.3 ± 6.1	68.1 ± 0.3

In the range 210–288 K, besides the exchange **a** ⇌ **b**, a decrease in species **6d** and **6e** and an increase in **6c** are observed, The largest concentration of **6c** is observed at 293 K. In other words, a dimer (**d**, **e**) to monomer (**c**) equilibrium is operative. Furthermore, at 293 K the equilibrium shifts almost completely towards **c** for all compounds **1**–**6**.

Below 288 K, the exchanges **a** ⇌ **c** ⇌ **b** are not observed. Conversely, EXSY experiments in the range 298–318 K clearly indicate that the exchange **b** ⇌ **c** is operative. In particular, Figure 4 shows the methylene exchange of **2** at 318 K (left-hand side) and that of **6** at 313 K (right-hand side).

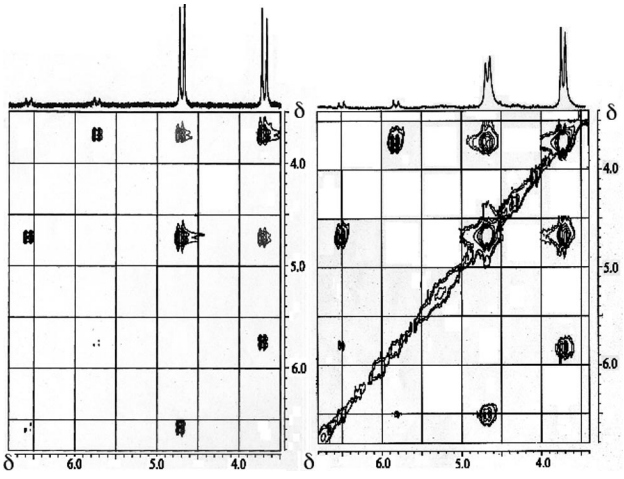

Figure 4. 300 MHz ^{1}H 2D EXSY NMR spectra in the methylene region of **2** at 318 K (left) and that of **6** at 313 K (right).

This dynamic behaviour allows us to deduce the rates of inversion at the sulfur centre by band-shape analysis of the methylene and methyl proton signals in the range 200–328 K, whereas the rates of the exchanges **b** ⇌ **c** are determined in the range 293–328 K.

The activation parameters, calculated by gNMR program and Eyring linear fitting, are listed in Table 2. The energy barriers for inversion at the sulfur centre are in the 50–53 kJ mol^{-1} range, whereas those for the higher-temperatures process are in the 64–68 kJ mol^{-1} range.

Examples of band-shape analysis in the range 210–288 K and in the range 293–328 K are depicted in Figures 5 and 6, respectively.

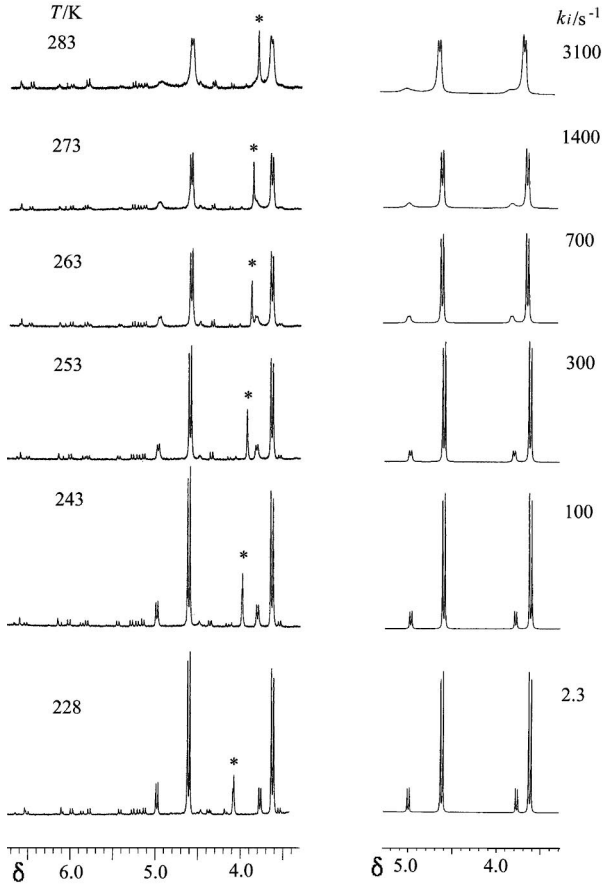

Figure 5. Variable-temperature 600 MHz ^{1}H NMR spectra of **6** in the methylene region; * denotes impurity band; computer-synthesized spectra (only major isomers **a** and **b**) are shown on the right.

The ^{13}C NMR spectra of mixtures **1**–**6** allowed almost all the carbon signals of the major isomer to be assigned by comparison of the spectra of these compounds with those of similar species[13–15,17] containing N,S-chelate ligands. The ^{13}C NMR spectra of **1** at 233 and 325 K are typically representative of the spectra for the compounds containing the pps ligand. Compound **1** exhibits carbon signals of the ancillary ligands, at 233 K, in the range δ = 158.0–155.0 (C^2 and C^6 pyridyl carbon atoms), 139.5–138.0 (C^4), 129.5–127.5 (C^3), 126.5 –124.5 (C^5) ppm. At 325 K,

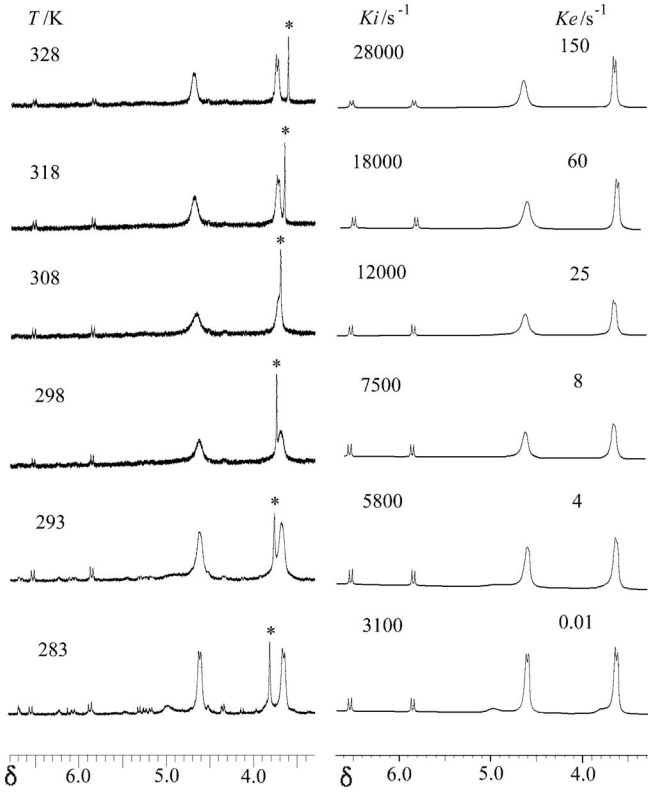

Figure 6. Variable-temperature 600 MHz ^{1}H NMR spectra of **6** in the methylene region; * denotes impurity band; computer-synthesized spectra (only isomers **a** + **b** and **c**) are shown on the right.

the corresponding signals are in the range δ = 160.5–157.0 (C^2 and C^6), 141.5–140.0 (C^4), 131.5–129.5 (C^3), 128.5–126.5 (C^5) ppm.

The C^5 pyrimidyl signals at 233 and 325 K are observed at δ = 121.1, 122.7 ppm, respectively, and the signals for the C^4 and C^6 equivalent carbon atoms are observed at δ = 157.8, 159.7 ppm. The picolyl carbon signals appear at δ = 155.9, 158.4 (C^6); 137.4, 139.4 (C^4); 122.9, 125.0 (C^5); 122.7, 124.8 (C^3) ppm.

Little information on the dynamic process was obtained from the ^{13}C NMR spectra in that generally the signals of minor species are not observed and the temperature has a negligible effect on the signals of major species. At 233 and 325 K, only the $C_{pirimidyl}$–S (166.1 and 171.4 ppm, respectively), C–CH_2 (164.1 and 167.9 ppm, respectively) and the methylene (43.6 and 46.0 ppm, respectively) signals of the major species are remarkably deshielded at high temperatures. In the spectra of compounds containing the mps ligand, the methyl carbon signals in the range δ = 22.0–24.0 ppm and the pyrimidine C–Me signals in the range δ = 166–169 ppm are observed.

Discussion

The crystal structures of [Ru(*N*,*N*-dps)$_2$(*N*,*S*-dps)]-[PF_6]$_2$,[13] [Ru(*N*,*N*-dps)$_2$(*N*,*S*-picolylpiridylsulfide)][PF_6]$_2$[15] and [Ru(*N*,*N*-dps)$_2$(*N*,*S*-mps)][PF_6]$_2$[16] showed, in addition to N,N-chelation of two molecules of dps, the N,S-coordination of the other ligand with the formation of the RuSCN(*Ru*-*N*) four-membered ring in [Ru(*N*,*N*-dps)$_2$(*N*,*S*-dps)][PF_6]$_2$[13] and the RuSCCN(*Ru*-*N*) five-membered ring in the other compounds.[15,16] Furthermore, because the trichelated ruthenium and the coordinated sulfur atoms are stereogenic centres, with Δ and Λ and *R* and *S* configurations, respectively, four isomers can exist (ΔR, ΛS, ΛR and ΔS).

1D and 2D NMR experiments, at variable temperatures, performed with [Ru(*N*,*N*-LL)$_2$(*N*,*S*-pySCH$_2$R)][PF_6]$_2$ and [Ru(*N*,*N*-LL)$_2$(*N*,*S*-prSCH$_2$R)][PF_6]$_2$ solutions[14] (LL = dps or dprs, py = pyridine, pr = pyrimidine and R = phenyl derivative) showed that the pyramidal inversion at the sulfur atom produced an exchange between the diastereoisomers ($\Delta R \rightleftharpoons \Delta S$, $\Lambda R \rightleftharpoons \Lambda S$). An intramolecular mechanism without any bond rupture was suggested on the basis of the $\Delta S^{\#}$ values (negative or close to zero) and the NMR spectra that were temperature reversible and concentration independent. The low values of $\Delta G^{\#}_{298}$ (50–55 kJ mol^{-1}) were explained in terms of the contemporary presence of the congested Ru(*N*,*N*-diimine)$_2$ fragment and the sterically demanding N,S-coordinated thioethers, which produced a high-energy ground state.

The potential tridentate thioethers L^1 reacted with Ru(*N*,*N*-diimmine)Cl_2 to give N,S-bidentate species of the type [Ru(*N*,*N*-diimmine)$_2$*N*,*S*-L^1][PF_6]$_2$ and, in certain cases, N-monodentate species of the type [Ru(*N*,*N*-diimmine)$_2$(solvent)*N*-L^1][PF_6].[17]

We proposed that, in the compounds, exchange occurred between the pendant pyrimidine ring and the coordinated sulfur atom, whereas the $N_{pyridine}$ atom was always coordinated to ruthenium, as a result of the ligand trying but failing to adopt tridentate bonding. This mechanism involves a seven-coordinate metal transition state in which the $N_{pyridine}$, S and $N_{pyrimidine}$ atoms contributed to the bonding, subsequent formation of the labile $N_{pyridine}$,$N_{pyrimidine}$ intermediate and fast dissociation and recoordination of the $N_{pyrimidine}$ atom. The $\Delta S^{\#}$ values (negative) reflected the formation of the seven-coordinate transition state, whereas the $\Delta G^{\#}_{298}$ values (ca. 59.5 kJ mol^{-1}), similar for all compounds, reflected the rupture of the Ru–S bond to form the N,N-intermediate.

The different Ru–$N_{pyridine}$, Ru–S and Ru–$N_{pyrimidine}$ bond strengths and the nature of the ancillary ligands likely favoured the mechanism. A simple dissociative mechanism involving rupture of the Ru–S bond in the N,S-chelated species was discarded not only in that the $\Delta S^{\#}$ value was negative, but also taking into account that (1) the process was clearly the same in acetone and acetonitrile below 345 K (above this temperature some decomposition occurred) and (2) the process was present only in the congested ruthenium cores with N,S-chelated ligands containing at least three donor atoms.

This paper explores the nature and the dynamic behaviour of the compound mixtures obtained by reaction of L with *cis*-[$RuCl_2$(*N*,*N*-L′)$_2$]. The species obtained contain L and the Ru(*N*,*N*-L′) unit in a ratio of 1:1. The major species have the formula [Ru(*N*,*N*-L′)$_2$(*N*,*S*-L)][PF_6]$_2$ [L′ = dps, L

= pps (**1**), mps (**2**); L′ = 4mdps, L = pps (**3**), mps (**4**); L′ = 5mdps, L = pps (**5**), mps (**6**)].

The NMR spectra at low temperatures of all the compounds obtained show that the major species (**a**) always exhibits the Δ*S* Λ*R* configuration, as observed in the solid state.[16] However, in solution, the Δ*R* Λ*S* (**b**) pair is also present, and inversion of the sulfur centre produces the exchange **a** ⇌ **b**.

The activation parameters are listed in Table 2. The $\Delta S^{\#}$ values for inversion at the sulfur centre are negative for complexes **2**, **3**, **5** and **6**. Thus, the transition-state conformations should be sterically even more congested than the ground state conformations, suggesting that a dissociative mechanism can be discarded. For compounds **1** and **4** the $\Delta S^{\#}$ values are close to zero but the $\Delta G^{\#}$ values (ca. 50.5 kJ mol^{-1}) are of comparable magnitude, which suggests that a similar mechanism is operative. Moreover, the $\Delta G^{\#}$ values of compounds **1**–**6** are comparable with those of $[Ru(N,N\text{-LL})_2(N,S\text{-pySCH}_2R)][PF_6]_2$[14] (LL = dps or dprs, py = pyridine, and R = phenyl derivative), in which an intramolecular mechanism without any bond rupture is operative for inversion of the sulfur centre.

Conversely, a mechanism involving the association of solvent molecules, anions or free ligands can be discarded by taking into account the following NMR findings: (1) The NMR spectra are temperature reversible and concentration independent at least in the range 210–288 K. (2) When free ligand is added, separate signals are observed and the exchange rates are not affected. (3) The addition of hexafluorophosphate anions does not affect the exchange rate.

The mechanism, therefore, which is consistent with all the experimental results, appears to be the pyramidal inversion without any bond rupture.

It is important to note that (1) in all the mixtures, the exchanges between **a** or **b** and dinuclear species are not observed, (2) below 288 K the exchanges **a** ⇌ **c** and **b** ⇌ **c** do not occur, (3) for the mixtures **1**, **2**, **5** and **6**, in the range 210–288 K, in addition to the exchange **a** ⇌ **b**, a decrease in the species **d**, **e** and an increase in **c**, which exhibits the biggest concentration in the range 288–293 K and at same time the dinuclear species disappear, are observed and (4) when the dinuclear species are not observed, **c** has the same abundance at low and high temperatures (5.0% **3**, 8.0% **4**).

These observations are in line with an equilibrium between the dinuclear (**d**, **e**) and mononuclear (**c**) species in all mixtures. When, in equilibrium, **c** largely predominates above 208 K (mixtures **3**, **4**) the dinuclear species are not observed, whereas when the dinuclear species (**d**, **e**) predominate in the range 208–288 K (mixtures **1**, **2**, **5**, **6**) **c** is in very low abundance.

The EXSY experiments in the range 298–318 K show that, at high temperatures, the exchange **b** ⇌ **c** occurs (Figure 4). Thus, we calculate the rates of inversion at the sulfur centre in the range 200–328 K (Figures 5 and 6) and those of the N–N exchanges **b** ⇌ **c** in the range 293–328 K (Figure 6).

The $\Delta S^{\#}$ values of the exchanges **b** ⇌ **c** are positive, which suggests that the transition state is less congested with respect to the ground state. The $\Delta G^{\#}$ values (62–68 kJ mol^{-1}) are bigger than those obtained for inversion at the sulfur centre for the same compounds and those of other processes studied for similar compounds.[14,17] We suppose that these $\Delta G^{\#}$ values reflect the rupture of the $Ru–N_{pyridine}$ bond, which was not observed previously. This may indicate a dissociative mechanism with formation of labile S-monodentate species and subsequent fast $N_{pyrimidine}$,S chelation as shown in Scheme 2. In other words, the $Ru–N_{pyrimidine}$ bond is not substantially made at the point where the $Ru–N_{pyridine}$ bond is broken to a considerable extent.

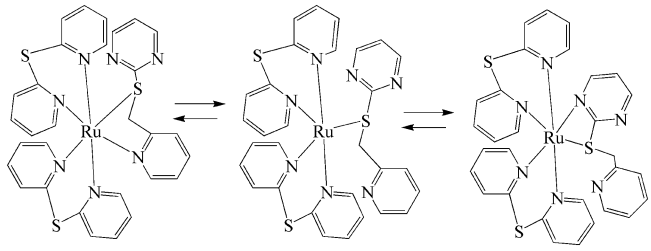

Scheme 2. Proposed mechanism of N,N-exchange.

On the other hand, an associative mechanism for **b** ⇌ **c** involving the solvent, the free ligand or the PF_6^- anion is unlikely in that (1) when the free ligand is added separate signals are observed and the exchange rates are not affected, (2) the addition of PF_6^- does not influence the exchange rate and (3) the exchange rates are concentration independent.

EXSY experiments (Figure 3) show that the reversible loss of the $N_{pyridine}$–ruthenium bond in the N,S-chelate species (**a**, **b**) does not occur below room temperature although the ^{1}H NMR spectra show the presence of the $N_{pyrimidine}$,S-chelate species in low abundance already at 208 K. Thus, at low temperatures, the $N_{pyrimidine}$,S-chelate species is formed only by dissociation of dinuclear species in the dimer monomer equilibria. The chelate effect, in the N,S-chelate species, likely makes the rupture of the $Ru–N_{pyridine}$ bond more difficult than the same process in the dinuclear species.

Conclusions

The reactions of *cis*-$RuCl_2$(dipyridyl sulfide)$_2$ or derivatives with thioethers based on pyridine and pyrimidine allowed us to obtain a mixture of ruthenium(II) species in which the coordinated thioether ligands undergo three processes: inversion at the sulfur centre, dimer to monomer equilibrium and $N_{pyridine}$,$N_{pyrimidine}$ switch. The inversion at the sulfur centre (**a** ⇌ **b**) and the dimer to monomer equilibrium (**a** ⇌ **c** ⇌ **b**) involve different species. Inversion at the sulfur centre and the N,N-exchange between $N_{piridine}$,S-chelated and $N_{pyrimidine}$,S-chelated occur at distinct rates, and the difference in the averaged $\Delta G^{\#}$ values is 13 kJ mol^{-1}.

According to NMR spectroscopic findings, inversion at the sulfur centre is an intramolecular process without bond rupture, whereas $N_{pyridine}$,$N_{pyrimidine}$ switching is likely to be a dissociative process, at least above room temperature.

Unfortunately, the limited quantities of dimer (**d**, **e**) and monomer (**c**) precluded measurement of the equilibrium constants. This problem could be resolved by synthesizing mixtures in which the quantities of species similar to **c**, **d** and **e** noticeably increase. We are currently engaged in such work.

Experimental Section

General remarks: Di-2-pyridyl sulfide (dps),[18] 2,2′-bis(4-methylpyridyl) sulfide (4mdps),[14] 2,2′-bis(5-methylpyridyl) sulfide (5mdps),[14] 2-pyridylmethyl 2′-pyrimidyl sulfide (pps),[17] 2-pyridylmethyl 2′-(4-methylpyrimidinyl) sulfide (mps),[17] $[Ru(dps)_2Cl_2]\cdot 2H_2O$,[13] $[Ru(4mdps)_2Cl_2]$[15] and $[Ru(5mdps)_2Cl_2]$[15] were prepared by published methods. Other reagents and solvents were used as received. All the syntheses were performed under N_2, and all the complexes were dried with P_4O_{10} under vacuum. Elemental analyses were carried out at the Redox Microanalytical Laboratory of Cologno Monzese (Milano). Conductivity measurements were performed with a Metrohm 644 conductometer. Infrared spectra were recorded with a Perkin–Elmer RX I FTIR spectrophotometer with samples as Nujol mulls placed between KBr plates. ^1H and ^{13}C NMR spectra were recorded with Bruker AMX 300 and AMX 600 spectrometers. Simulations of static and dynamic spectra were performed by using the gNMR program.

$[Ru(dps)_2(psp)][PF_6]_2$ (1): $[RuCl_2(dps)_2]\cdot 2H_2O$ (0.195 g, 0.33 mmol) and 2-pyridylmethyl 2-pyrimidyl sulfide (0.178 g, 0.882 mmol) were heated to reflux in ethanol/water (3:2, 50 mL) for 4 h. After filtration of the solution into water (50 mL) containing NH_4PF_6 (0.98 g, 6.0 mmol) an orange precipitate was obtained, which was filtered, washed with water and dried overnight. The solid was dissolved in acetone (15 mL), precipitated with diethyl ether (100 mL) and washed with diethyl ether (50 mL). Yield: 0.194 g (60%). IR (KBr): $\tilde{\nu}$ = 1594 (s), 1559 (s), 1556 (s), 1552 (s), 1286 (s), 1159 (s), 879 (s), 840 (br.), 773 (vs), 767 (vs), 744 (s), 558 (vs) cm^{-1}. $C_{30}H_{25}F_{12}N_7P_2RuS_3$ (970.76): calcd. C 37.12, H 2.59, N 10.10; found C 37.90, H 2.65, N 10.00. Conductivity: Λ_M (MeCN, 2×10^{-4} mol L^{-1}, 25 °C) = 335 S cm^2 mol^{-1}.

$[Ru(dps)_2(msp)][PF_6]_2$ (2): According to the above procedure a yellow-orange compound was obtained from $[RuCl_2(dps)_2]\cdot 2H_2O$ (0.195 g, 0.33 mmol) and 2-pyridylmethyl 2′-(4methylpyrimidyl sulfide (0.192 g, 0.885 mmol). Yield: 0.197 g (60%). IR (KBr): $\tilde{\nu}$ = 1607 (ms), 1581 (s), 1577 (vs), 1534 (ms), 1285 (ms), 1165 (s), 1089 (s), 876 (vs), 844 (br.), 768 (vs), 727 (s), 558 (vs) cm^{-1}. $C_{31}H_{27}F_{12}N_7P_2RuS_3$ (984.15): calcd. C 37.81, H 2.76, N 9.96; found C 38.00, H 2.85, N 9.90. Conductivity: Λ_M (MeCN, 2×10^{-4} mol L^{-1}, 25 °C) = 330 S cm^2 mol^{-1}.

$[Ru(4mdps)_2(psp)][PF_6]_2$ (3): According to the above procedure a yellow-orange compound was obtained from $[RuCl_2(4mdps)_2]$ (0.202 g, 0.33 mmol) and 2-pyridylmethyl 2-pyrimidyl sulfide (0.178 g, 0.882 mmol). Yield: 0.222 g (65%). IR (KBr): $\tilde{\nu}$ = 1606 (vs), 1556 (vs), 1291 (s), 1161 (s), 1092 (s), 874 (vs), 844 (br.), 776 (s), 740 (s), 723 (ms), 558 (vs) cm^{-1}. $C_{34}H_{33}F_{12}N_7P_2RuS_3$ (1026.87): calcd. C 39.77, H 3.24, N 9.55; found C 39.85, H 3.30, N 9.50. Conductivity: Λ_M (MeCN, 2×10^{-4} mol L^{-1}, 25 °C) = 320 S cm^2 mol^{-1}.

$[Ru(4mdps)_2(msp)][PF_6]_2$ (4): According to the above procedure a yellow-orange compound was obtained from $[RuCl_2(4mdps)_2]$ (0.202 g, 0.33 mmol) and 2-pyridylmethyl 2′-(4methylpyrimidyl sulfide (0.192 g, 0.885 mmol). Yield: 0.222 g (65%). IR (KBr): $\tilde{\nu}$ = 1605 (vs), 1573 (vs), 1535 (s), 1291 (s), 1090 (s), 874 (vs), 841 (br.), 779 (vs), 740 (s), 721 (s), 558 (vs) cm^{-1}. $C_{35}H_{35}F_{12}N_7P_2RuS_3$ (1040.90): calcd. C 40.39, H 3.39, N 9.42; found C 40.60, H 3.45, N 9.40. Conductivity: Λ_M (MeCN, 2×10^{-4} mol L^{-1}, 25 °C) = 320 S cm^2 mol^{-1}.

$[Ru(5mdps)_2(psp)][PF_6]_2$ (5): According to the above procedure a yellow-orange compound was obtained from $[RuCl_2(5mdps)_2]$ (0.202 g, 0.33 mmol) and 2-pyridylmethyl 2-pyrimidyl sulfide (0.178 g, 0.882 mmol). Yield: 0.222 g (65%). IR (KBr): $\tilde{\nu}$ = 1608 (s), 1598 (s), 1555 (vs), 1284 (s), 1240 (s), 1161 (vs), 1121 (s), 1089 (s), 873 (vs), 840 (br.), 775 (vs), 740 (s), 724 (ms), 558 (vs), 530 (vs) cm^{-1}. $C_{34}H_{33}F_{12}N_7P_2RuS_3$ (1026.87): calcd. C 39.77, H 3.24, N 9.55; found C 39.80, H 3.30, N 9.50. Conductivity: Λ_M (MeCN, 2×10^{-4} mol L^{-1}, 25 °C) = 345 S cm^2 mol^{-1}.

$[Ru(5mdps)_2(mpsp)][PF_6]_2$ (6): According to the above-mentioned procedure a yellow-orange compound was obtained from $[RuCl_2(5mdps)_2]$ (0.202 g, 0.33 mmol) and 2-pyridylmethyl 2′-(4-methylpyrimidyl) sulfide (0.192 g, 0.885 mmol). Yield: 0.222 g (65%). IR (KBr): $\tilde{\nu}$ = 1577 (vs), 1533 (s), 1283 (s), 1179 (s), 1121 (s), 874 (vs), 844 (br.), 774 (vs), 740 (s), 722 (s), 714 (ms), 558 (vs), 530 (vs) cm^{-1}. $C_{35}H_{35}F_{12}N_7P_2RuS_3$ (1040.90): calcd. C 40.39, H 3.39, N 9.42; found C 40.50, H 3.45, N 9.40. Conductivity: Λ_M (MeCN, 2×10^{-4} mol L^{-1}, 25 °C) = 350 S cm^2 mol^{-1}.

Supporting Information (see footnote on the first page of this article): Selected ^1H and ^{13}C NMR spectroscopic data and spectra.

Acknowledgments

We are grateful to MIUR for financial support (PRIN 2005 n. 2005033820_004).

[1] a) E. C. Constable, R. P. G. Henney, D. A. Tocher, *J. Chem. Soc., Dalton Trans.* **1991**, 2335–2347; b) R. Chotalia, E. C. Constable, M. J. Hannon, D. A. Tocher, *J. Chem. Soc., Dalton Trans.* **1995**, 3571–3580; c) F. G. de la Torre, A. de la Hoz, F. A. Jalòn, B. R. Manzano, A. M. Rodrìguez, J. Elguero, M. Martìnez-Ripoll, *Inorg. Chem.* **2000**, *39*, 1152–1162.

[2] J. H. Groen, P. W. N. M. van Leeuwen, K. Vrieze, *J. Chem. Soc., Dalton Trans.* **1998**, 113–117.

[3] A. Gelling, M. D. Olsen, K. G. Orrell, A. G. Osborne, V. Sik, *J. Chem. Soc., Dalton Trans.* **1998**, 3479–3488.

[4] P. J. Heard, *Chem. Soc. Rev.* **2007**, *36*, 551 –569.

[5] a) C. S. Slone, D. A. Weinberger, C. A. *Mirkin*, *Prog. Inorg. Chem.* **1999**, *48*, 233–350; b) P. Braunstein, F. Naud, *Angew. Chem. Int. Ed.* **2001**, *40*, 680–699.

[6] a) E. W. Abel, K. G. Orrell, A. G. Osborne, H. M. Pain, V. Sik, *J. Chem. Soc., Dalton Trans.* **1994**, 111–116; b) P. J. Heard, C. Jones, *J. Chem. Soc., Dalton Trans.* **1997**, 1083–1091; c) P. J. Heard, D. A. Tocher, *J. Chem. Soc., Dalton Trans.* **1998**, 2169–2176.

[7] a) E. W. Abel, V. S. Dimitrov, N. J. Long, K. G. Orrell, A. G. Osborne, H. M. Pain, V. Sik, M. B. Hursthouse, M. A. Mazid, *J. Chem. Soc., Dalton Trans.* **1993**, 291–298; b) E. W. Abel, V. S. Dimitrov, N. J. Long, K. G. Orrell, A. G. Osborne, H. M. Pain, V. Sik, M. B. Hursthouse, M. A. Mazid, *J. Chem. Soc., Dalton Trans.* **1993**, 597–603.

[8] E. W. Abel, K. G. Orrell, A. G. Osborne, V. Sik, M. B. Hursthouse, K. M. A. Malik, *J. Chem. Soc., Dalton Trans.* **1994**, 3441–3449.

[9] E. W. Abel, S. K. Bhargava, K. G. Orrell, *Prog. Inorg. Chem.* **1984**, *32*, 1–118.

[10] a) D. Parker, J. M. Lehn, J. Rimmer, *J. Chem. Soc., Dalton Trans.* **1985**, 1517–1521; b) E. W. Abel, D. Ellis, K. G. Orrell, *J. Chem. Soc., Dalton Trans.* **1992**, 2243–2249; c) E. W. Abel, P. J. Heard, K. G. Orrell, M. B. Hursthouse, M. A. Mazid, *J. Chem. Soc., Dalton Trans.* **1993**, 3795–3801; d) E. W. Abel, E. S. Blackwoll, M. L. Creber, P. J. Heard, K. G. Orrell, *J. Organomet. Chem.* **1995**, *490*, 83–88.

[11] a) E. W. Abel, N. J. Long, K. G. Orrell, A. G. Osborne, H. M. Pain, V. Sik, *J. Chem. Soc., Chem. Commun.* **1992**, 303–304; b) E. Rotondo, G. Giordano, D. Minniti, *J. Chem. Soc., Dalton Trans.* **1996**, 253–254; c) M. L. Creber, K. G. Orrell, A. G. Osborne, V. Sik, M. B. Hursthouse, K. M. A. Malik, *J. Chem. Soc., Dalton Trans.* **2000**, 4218–4226.

[12] a) G. Tresoldi, P. Piraino, E. Rotondo, F. Faraone, *J. Chem. Soc., Dalton Trans.* **1991**, 425–430; b) G. Tresoldi, E. Rotondo, P. Piraino, M. Lanfranchi, A. Tiripicchio, *Inorg. Chim. Acta* **1992**, *194*, 233–241; c) G. De Munno, G. Bruno, E. Rotondo, G. Giordano, S. Lo Schiavo, P. Piraino, G. Tresoldi, *Inorg. Chim. Acta* **1993**, *208*, 67–75; d) G. Bruno, F. Nicolò, S. Lo Schiavo, M. S. Sinicropi, G. Tresoldi, *J. Chem. Soc., Dalton Trans.* **1995**, 17–24; e) G. Tresoldi, S. Lo Schiavo, P. Piraino, P. Zanello, *J. Chem. Soc., Dalton Trans.* **1996**, 885–892; f) F. Nicolò, G. Bruno, G. Tresoldi, *Acta Crystallogr., Sect. C* **1996**, *52*, 2188–2191 ; g) G. Tresoldi, S. Lo Schiavo, P. Piraino, *Inorg. Chim. Acta* **1997**, *254*, 381–385; h) G. Bruno, F. Nicolò, G. Tresoldi, *Acta Crystallogr., Sect. C* **2000**, *56*, 282–283.

[13] R. Scopelliti, G. Bruno, C. Donato, G. Tresoldi, *Inorg. Chim. Acta* **2001**, *313*, 43–55.

[14] G. Tresoldi, S. Lo Schiavo, S. Lanza, P. Cardiano, *Eur. J. Inorg. Chem.* **2002**, 181–191.

[15] L. Baradello, S. Lo Schiavo, F. Nicolò, S. Lanza, G. Alibrandi, G. Tresoldi, *Eur. J. Inorg. Chem.* **2004**, 3358–3369.

[16] G. Bruno, A. Rotondo, G. Tresoldi, F. Nicolò, S. Lanza, *Acta Crystallogr., Sect. C* **2005**, *61*, M169–M172.

[17] G. Tresoldi, L. Baradello, S. Lanza, P. Cardiano, *Eur. J. Inorg. Chem.* **2005**, 2423–2435.

[18] C. Chachaty, C. Pappalardo, C. G. Scarlata, *J. Chem. Soc. Perkin Trans. 2* **1976**, 1234–1238.

Received: June 13, 2008
Published Online: September 16, 2008

